ORIGINAL RESEARCH PAPER
Pages: 305-317

A Miniaturized Fractal Defected Ground Structure Super-Widedband Antenna for Wireless Communication Systems

A. Dastranj[1] and Z. Javidi[2]
1.Electrical Engineering Depart., Faculty of Engineering, Yasouj University, Yasouj 75918-74831, Iran.
2.College of Electrical Engineering, Iran University of Science and Technology, Tehran, Iran.
dastranj@yu.ac.ir, jazahviradi@gmail.com
Corresponding author: *dastranj@yu.ac.ir*

DOI: 10.22070/JCE.2023.17853.1249

Abstract- A low profile fractal defected ground structure (DGS) antenna is presented for super-wideband (SWB) wireless communication applications. The designed antenna covers a very wide frequency range from 1 to 27.4 GHz (impedance bandwidth of 186%) with |S11|<-10 dB. Moreover, In spite of small electrical dimension of the proposed antenna (0.11 λ× 0.11 λ), a large bandwidth dimension ratio of 15372 is resulted. The SWB operation is achieved by using fractal DGS on the ground plane to improve the impedance characteristics between adjacent resonant frequencies. The antenna consists of a 34×34×1.6 mm3 FR4 substrate with a dielectric constant of 4.4 and a narrow rectangular radiator. A multi-frequency resonance characteristic is obtained by increasing the fractal slot iterations on the ground plane. The simulation results are verified by experimental measurements. Measured data are in good agreement with the simulated results. The frequency- and time-domain characteristics of the antenna including impedance matching, far-field patterns, gain, radiation efficiency, group delay, and fidelity factor are presented and discussed. The results indicate that the antenna has good performance over the entire operating bandwidth which make it very potential candidate for integration in SWB wireless communication systems.

***Index Terms*-** Direction of arrival (DoA) estimation, coherent sources, uniform circular array (UCA), beamspace transformation (BT), bias reduction.

I. INTRODUCTION

Direction of arrival (DoA) estimation is one of the most important research areas in array signal processing which has so many applications in localization, tracking, surveillance, and navigation [1-4]. Sub-space based DoA estimation methods, such as MUSIC [5] and ESPRIT [6] which are based on the Eigen structure of the received vector covariance matrix are the most powerful methods for

Manuscript received 15-March-2021 and revised 11-May-2021, *P-ISSN: 2322-4088*
Accepted on 13- June-2021 *E-ISSN:2322-3936*

DoA estimation. However, these methods are unable to estimate the DoA of coherent sources. At the presence of coherent sources, the source covariance matrix is not full-ranked (is rank deficient). Some modified methods have been proposed for DoA estimation of coherent sources in uniform linear arrays (ULAs) such as: Spatial Smoothing (SS) [7-10], reconstruction of the Toeplitz structure of covariance matrix [11-12], Spatial Differencing (SD) [13], $M\ell_{1,2}$-MUSIC [14], and Beamspace matrix reconstruction [15].

Printed fractal antennas have attracted much attention in wireless communication because of their low profile, small cost, and ease of manufacture [3]. These antennas have shown the possibility to miniaturize antenna systems and to improve input impedance matching. Also, a fractal antenna can be designed to operate over a wide range of frequencies using the self-similarity properties associated with fractal geometry structures. Planar fractal antennas can be used in variety of wideband applications, especially where space is limited. The geometry of fractal antenna was defined by Mandelbort in 1975 [4]. A fractal is a self-similar geometric shape of the whole structure which can be subdivided into the parts; each of the part is a reduced size copy of the whole geometry of the antenna [5]. Fractal geometry has some advantages over simple planar radiator such as: at arbitrarily minute scale it has an excellent structure, it can be easily described in traditional Euclidean geometry by using its irregular shape, simple and recursive, improving input resistance of antennas, and enhance electrical area [6]. Thus, to miniaturize the antenna size with high radiation efficiency, fractal antennas are most suitable [7].

In the recent years, to satisfy the broadband communication systems requirements, several investigations on fractal antennas have been reported [8]-[12]. In [8], a fractal monopole antenna with a volume of 24×24×1 mm3 can cover a bandwidth of 2.1–11.52 GHz. In [9], a CPW-fed octagonal Sierpinski fractal antenna can cover a bandwidth of 3.73–20 GHz. A multiband Koch-like sided fractal bow-tie dipole antenna was reported in [10]. The fractal printed bow-tie antenna in [11] can cover bandwidth from 1.64 to 1.94 GHz. In [12], an antenna with notch¬ band characteristics that uses koch fractal for UWB applications was proposed. Different fractal antennas for wideband application were reported in [13]-[15]. In [13], a circular-hexagonal fractal antenna was investigated for many wireless communications systems such as ISM, Wi-Fi, GPS, Bluetooth, WLAN, and UWB. It was made of iterations of a hexagonal slot inside a circular metallic patch with a transmission line. A partial ground plane and asymmetrical patch toward the substrate were used for designing the antenna to achieve a wide bandwidth. In [14], a hexagonal shaped fractal antenna with triangular slot and a total size of 20 × 33.4 × 1.57 mm3 for wideband application was presented. In [15], a printed star-triangular fractal microstrip-fed monopole antenna with semi-elliptical ground plane was presented for wideband applications. A miniaturized UWB antenna based on Sierpinski square slots was reported in [16]. It has a compact dimension of only 28 × 28 mm2 and a fractional bandwidth of about 127.3% (3.41-15.37 GHz). A printed Koch Snowflake antenna with an operating frequency

range of (3.4–16.4GHz for UWB radio frequency identification applications was presented in [17].

The miniaturized SWB antenna with a large bandwidth dimension ratio (BDR) can be found in few papers because having compact size and an extremely large BW with stable radiation characteristic at higher frequencies is very challenging [18]. In [19], a circular shape fractal antenna with BW ratio of 7.2:1 was presented. In [20], a dual band-notched SWB coplanar waveguide (CPW)-fed antenna with electrical dimension of 0.18 λ× 0.13 λ, BW ratio of 14.28:1 and operating BW of 173.8% was proposed. In [21], the antenna has a very large electrical dimension of 0.45 λ × 0.45 λ and BW of 1.0-19.4 GHz with a very low BDR. In addition, the antenna presented in [22] has a BW ratio of 10.16:1 and electrical dimension of 0.47 λ × 0.32 λ which is large in size compared to the BW the antenna provides. A CPW-fed hexagonal Sierpinski fractal radiator for SWB applications with the electrical dimension of 0.32 λ × 0.34 λ is introduced in [23] which has a BW ratio of 11:1. In [24], a monopole antenna fed by microstrip line with a BW ratio of 13:1 and electrical dimension of 0.17 λ × 0.37 λ has been proposed which has some radiation characteristic problems. The antenna presented in [25] has a low BDR due to its large electrical dimension of 0.35 λ × 0.20 λ compare to the BW of 3-35 GHz which the antenna can provide. Also, a set of SWB antennas were presented in [26]-[32] which will be compared to the proposed structure in section 3.

The work presented in this research is a miniaturized SWB printed antenna with electrical dimension of 0.11 λ× 0.11 λ (overall dimension of 34×34×1.6 mm^3), BW ratio of 27.4:1 and operating BW of 186%. Another important issue is to keep the antenna inexpensive and easy to manufacture. These goals are accomplished by using fractal defected ground structure (DGS) on the ground plane. The multi-frequency resonance characteristic is obtained by increasing the fractal slot iterations on the ground plane. The antenna has been simulated by full-wave Ansys Electromagnetics simulator package. The measured results of the fabricated prototype in frequency-and time-domain are also presented and compared with the simulated results. The proposed antenna has desirable performance based on the achievement results in both simulation and measurement. The performance of the designed antenna is compared with several recent SWB antennas. In spite of small electrical dimension of the antenna compare to the others, a large BDR of 15372 is provided. The results indicate that the antenna is an excellent choice for use in SWB wireless communication systems. The novelty of the proposed antenna lies in its simple structure, compact size, high BDR, and SWB operation. The antenna design and the process of reaching the final structure will be discussed in the following sections.

II. ANTENNA DESIGN AND EVOLUTION PROCEDURE

Fig. 1 presents the detailed configuration and fabricated prototypes of the proposed antenna. It is etched on 1.6 mm thick FR-4 epoxy (εr =4.4, $\tan\delta$ = 0.02) substrate. The copper cladding's thickness

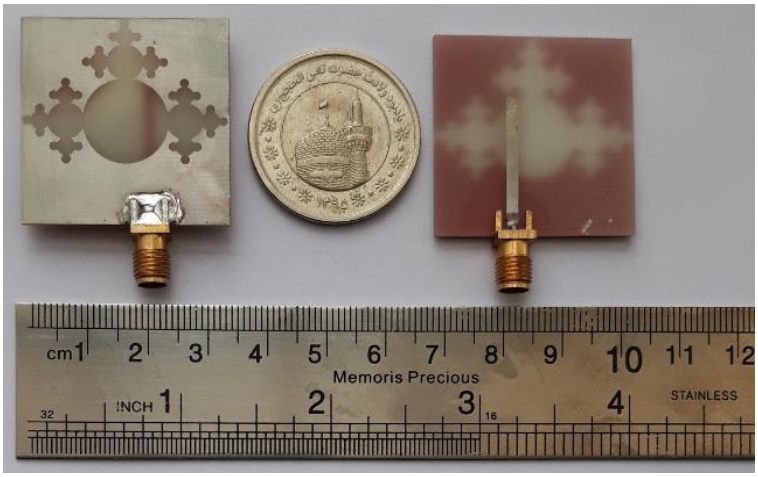

(a)

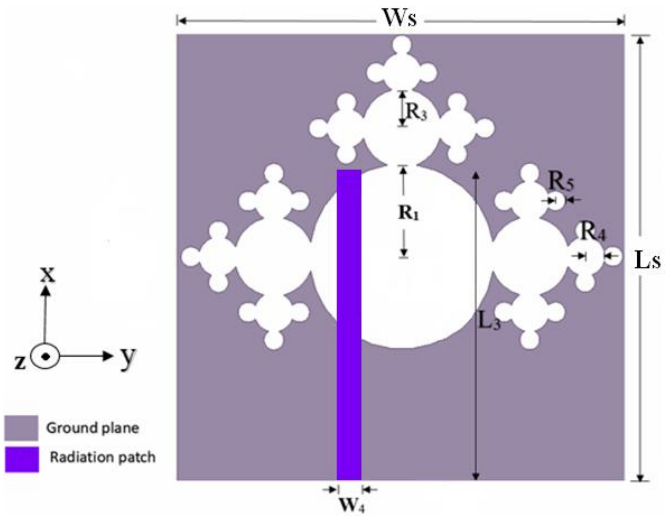

(b)

Fig. 1. (a) Fabricated prototypes of the antenna, (b) Antenna geometry and design parameters.

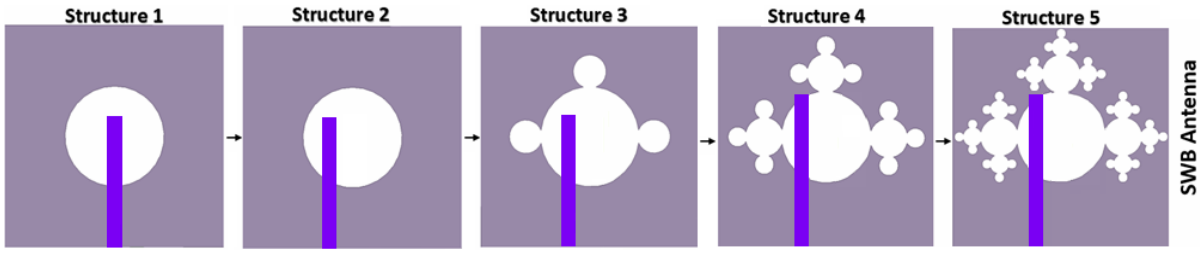

Fig. 2. Antenna evolution procedure.

and the electrical size of the antenna are 35μm and 0.11 λ × 0.11 λ, respectively.

A narrow rectangular line is used as microstrip feeding section and radiating patch. As shown in this figure, the feed-line is located asymmetrical with respect to the center of the substrate. Defected ground structure (DGS) technique including three iterations of fractal circular slots on the ground plane is used to achieve multi-frequency resonance characteristic, and consequently SWB operation. The development stages of the proposed antenna are illustrated in Fig. 2 and the corresponding simulated reflection coefficient curves are plotted in Fig. 3. The numerical analysis and geometry refinement of the proposed structure are performed by using Ansys Electromagnetics, a full-wave

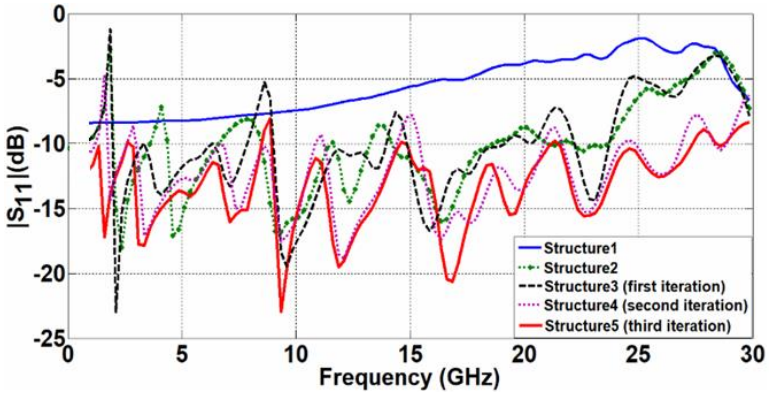

Fig. 3. Simulated reflection coefficient curves of the antennas corresponding to Fig. 2.

electromagnetic simulator package which is based on the finite element method. The design procedure starts with the design of structure1. As shown in Fig. 2, structure1 consists of a common microstrip line with 50Ω impedance, square ground plane which is loaded by a circular slot. Referring to Fig. 2, it can be observed that structure1 exhibits $|S_{11}|$> -10 dB over the entire frequency range. In the second structure, the microstrip line is displaced to the left side of the substrate. As a result, multi-band operation over 2-17GHz is obtained. In the next step, the first iteration of circular slots are etched on the ground plan, and as depicted in Fig. 2, structure3 exhibits two resonances in the reflection coefficient at 2 and 9.5 GHz whereas the structure2 does not. Afterwards, to improve the impedance characteristics between adjacent resonant frequencies, the second iteration of slots is loaded (structure4). In the last step of the antenna design (structure5), multi-frequency resonance characteristic is obtained by increasing the fractal slots iterations on the ground plane (up to three iterations). As illustrated in Fig. 2, for structure5 the lower and higher band edge frequencies of the operating bandwidth are shifted from 2 to 1 GHz and 22 to 27.4 GHz, respectively. This technique increases bandwidth, both at the beginning and end of the frequency band. Structure5 is the final proposed SWB antenna. It is observed in Fig. 2 that the proposed antenna features good impedance matching over the entire frequency range of 1-27.4 GHz. The relationship between the radii of the circular slots in fractal iterations according the parameters in Fig. 1(b) is as follows:

$$R_3 = 3mm, \quad R_4 = \frac{R_3}{3}, \quad R_5 = \frac{R_4}{2} \tag{1}$$

The optimized geometrical parameters of the proposed antenna (in mm) are as follows: Ws=34, Ls=34, W4=2.9, R1=7, R3=3, R4=1, R5=0.5, and L3=23.5.

Numerical parametric analysis via Ansys Electromagnetics was performed to understand the influence of the antenna physical dimensions on the impedance bandwidth. It was found that strip length, L3, and radius of the firs circular slot on the ground plane, R1, have considerable influence on the SWB performance of the proposed antenna. Reflection coefficient curve for two important parameters is shown in Fig. 4. As depicted in Fig. 4(a), the radius of the first circular slot affects the

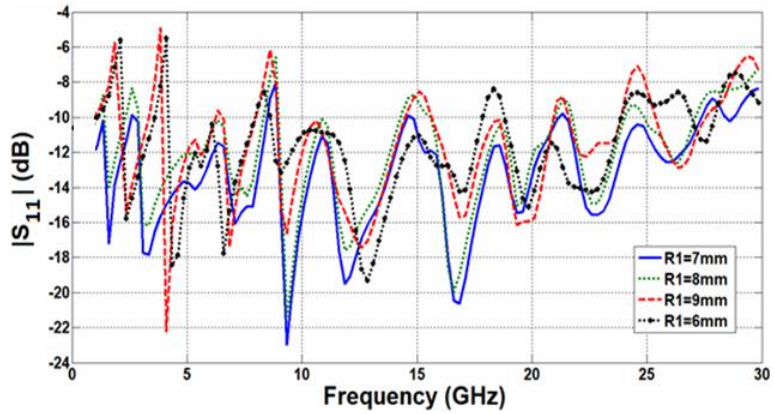

(a)

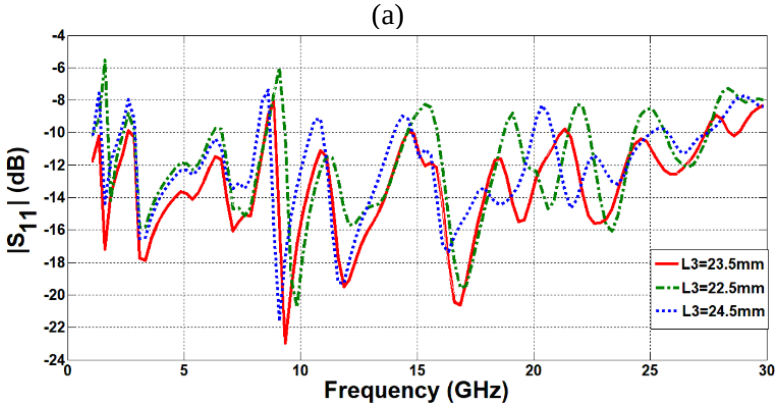

(b)

Fig. 4. Influence of R1 and L3 on the impedance bandwidth of the antenna (a) R1, (b) L3.

antenna reflection coefficient over the entire SWB spectrum. It is seen that the resonance frequencies of the antenna at 2, 4, 7, 9, 12, 17, and 23 GHz are largely depend on R1. The influence of variation of rectangular strip length L3 is presented in Fig. 4(b) while other geometrical parameters are kept fixed. It can be observed that this parameter influences the reflection coefficient at lower, middle, and higher frequencies. Results of Fig. 4 show that selecting the optimal values of R1 =7 mm and L3=23.5 mm leads to maximum impedance bandwidth.

III. FREQUENCY- AND TIME-DOMAIN RESULTS AND DISCUSSION

In order to validate the numerical results obtained by Ansys Electromagnetics, the designed fractal DGS SWB antenna was constructed and tested. Fig. 1(a) illustrates the photograph of the fabricated prototypes. The designed antenna is connected to a 50Ω SMA connector for signal transmission. The part number of SMA female connector is SC8026 which normally operates from DC up to a frequency of 18 GHz and offers excellent voltage standing wave ratio (VSWR) of 1.23:1. However, this connector features VSWR of about 1.45:1 for frequency range of 18-40 GHz. It is a low cost connector with reasonable lose. In the following, the experimental outcomes are given, discussed, and compared with the numerical results.

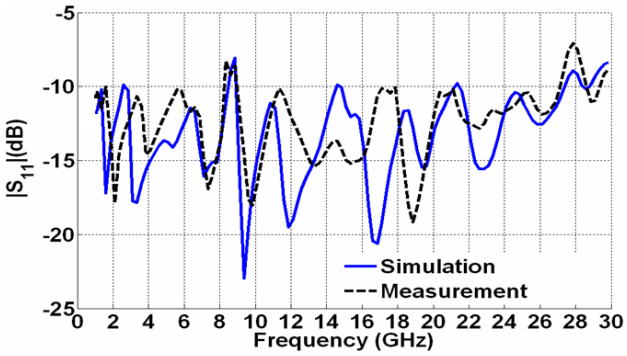

Fig. 5. Numerical and experimental reflection coefficient curves of the antenna

A) Frequency-domain results

Fig. 5 presents the comparison of experimental and numerical reflection coefficient curves of the proposed antenna. Measured and simulated results show that the designed fractal antenna can cover a SWB frequency range, from 1 to 27.4 GHz (186% impedance bandwidth). As shown in this figure, the scattering parameter (|S11|) at some part of frequency band between 8 to 9 GHz goes slightly greater than -10dB. There is a difference between the experimental and numerical results due to the measurement errors, fabrication tolerances, and SMA soldering effects. In order to further understand the utility of the proposed antenna over the entire operating bandwidth, other radiation characteristics such as far-field patterns, realized gain, and radiation efficiency must also be carefully investigated. The far-field radiation patterns of the antenna were measured at different frequencies. For brevity, the numerical and experimental E (x-z)- and H (y-z)-plane patterns at only 3, 5, 13, 20, and 27 GHz are compared in Fig. 6. A good concordance between the numerical and experimental outcomes is observed. As illustrated in this figure, the antenna features nearly omnidirectional patterns specifically in the x-z plane. In the desired application, such as mobile and indoor deployments, omnidirectional radiation pattern is needed. The fluctuations in the radiation pattern in different figures, especially Fig. 6(e) is due to excitation of higher order modes at higher frequencies. Fig. 7 plots the simulated and measured gain and radiation efficiency curves of the proposed antenna versus frequency. As shown in Fig. 7(a), the maximum value of the measured antenna gain is 6.2 dBi which occurs at 26 GHz. The measured gain has an average value of 3.18 dBi. It should be noted that the antenna gain is moderate over the working band respecting the compact size and omnidirectional behavior of the antenna. Besides, as shown in Fig. 7(b), the designed antenna can provide desirable radiation efficiency of greater than 80% over the frequency range of 1-16 GHz. The decrease in antenna radiation efficiency at higher frequencies, 16-27 GHz, is due to lossy FR4 substrate with loss tangent of 0.02.

In SWB antennas, BDR is an important parameter that the higher BDR signifies wider frequency band and compactness of the proposed antenna compare to the other structures. BDR indicates how much operating bandwidth (in percentage) can be provided per electrical area unit. The equality is defined as follows [20] and [24]:

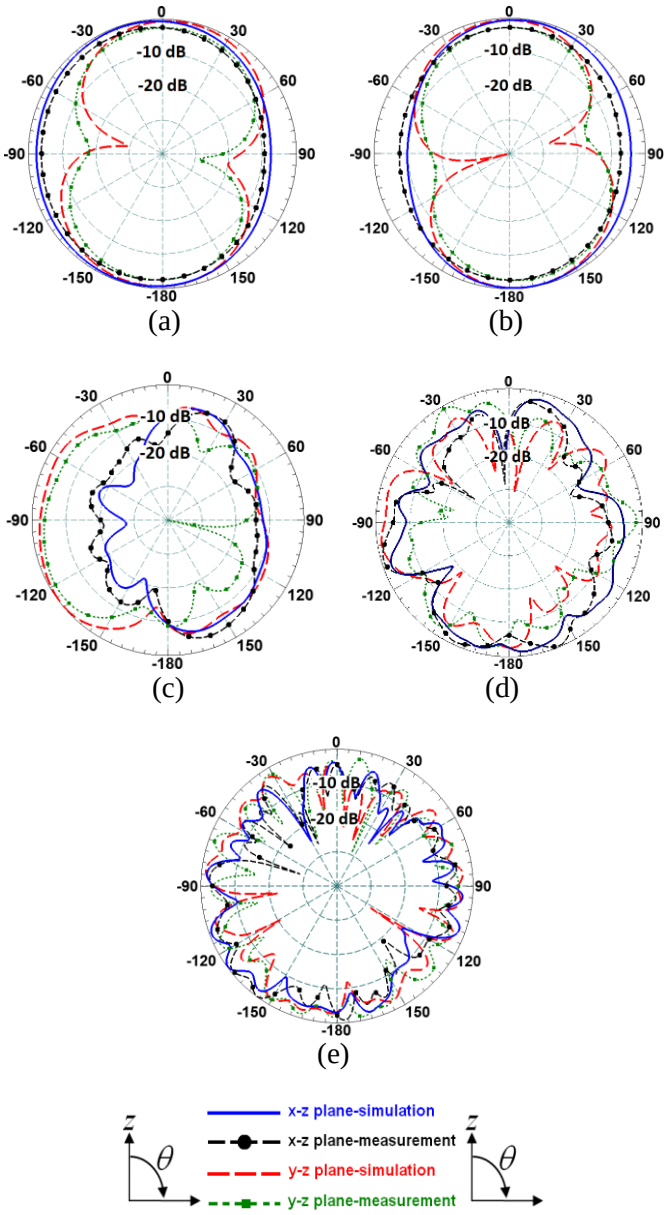

Fig. 6. Experimental and numerical far-field E (x-z)-and H (y-z)-plane patterns of the antenna, (a) 3 GHz, (b) 5 GHz, (c) 13 GHz, (d) 20 GHz, and (e) 27 GHz.

$$BDR = \frac{BW(\%)}{\lambda_{Length} \times \lambda_{Width}} \tag{2}$$

In this equation, λ is the wavelength at the lower cut-off frequency of the working BW. The results of the comparison between the designed antenna and other SWB antenna structures studied in [20-32], are presented in Table I on the basis of BDR. In spite of small electrical dimension of the proposed antenna compare to the others, a large BDR of 15372 is exhibited. Accordingly, it can be concluded that the proposed SWB antenna can provide good BW ratio and very larger BDR characteristics with much smaller size in comparison to the other antennas.

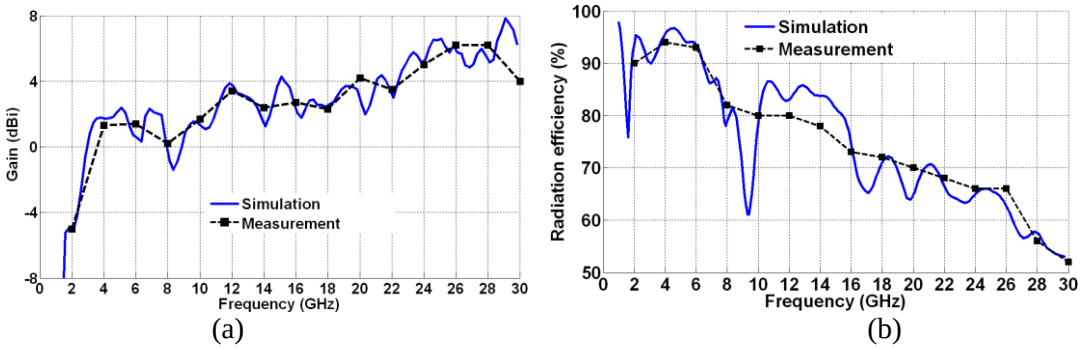

Fig. 7. Numerical and experimental radiation parameters of the antenna versus frequency. (a) Gain. (b) Radiation efficiency.

Table I. Comparison of the proposed antenna with others SWB antennas (AG: average gain, GD: group delay). Note that the electrical dimension and the BDR are calculated at the wavelength at the lower cut-off frequency of the working BW.

Ref.	Electrical dimension (λ^2)	BDR	ε_r	BW ratio	AG (dBi)	GD (ns)
[20]	0.18×0.13	7427.40	4.4	14.28:1	2.96	< 2
[21]	0.45×0.45	890.83	4.4	19.40:1	0.94	-----
[22]	0.47×0.32	1102.91	3.24	10.16:1	-4.8	-----
[23]	0.32×0.34	1531.89	4.4	11.00:1	6.1	-----
[24]	0.17×0.37	2735.00	4.4	13.06:1	4.1	-----
[25]	0.35×0.20	2400.00	2.2	11.60:1	5.8	-----
[26]	0.23×0.32	2230.00	-----	10.31:1	3.3	-----
[27]	0.41×0.29	1347.24	3.38	9.11:1	2.93	< 1
[28]	0.44×0.44	905.00	3.0	13.63:1	-----	-----
[29]	2.00×2.00	33.33	4.5	5.00:1	3.4	-----
[30]	0.32×0.34	1682.00	2.65	25.00:1	4.9	< 5
[31]	0.43×0.45	950.77	3.48	25.00:1	4.5	-----
[32]	0.27×0.23	2541.12	4.4	10.00:1	3.4	<0.7
Proposed	**0.11×0.11**	**15372**	**4.4**	**27.4:1**	**3.18**	**< 1**

B) Time-domain results

Along with frequency-domain analysis, time-domain performance should also be analysed in order to be sure of the SWB operation. The time-domain analysis required two identical designed antennas, one as the transmitter and the other one as a receiver, in the adjustment of face-to-face and side-by-side. Time-domain analysis of both configurations was considered using CST Microwave Studio by a distance of 50 cm. Time taken by the antenna to receive the pulse is indicated by an important parameter named group delay. In order to provide desirable time-domain behavior in a typical SWB system, constant group delay is required over the entire working band [33-36]. Group delay of side-by-side orientation is shown in Fig. 8 which its peak-to-peak variation is less than 1ns over the entire frequency band. Although the result of the face-to-face configuration has not been discussed in this section, similar results were obtained which indicate an acceptable time-domain performance.

Another important parameter in time-domain analysis named the fidelity factor is used to calculate the correlation between transmitted and received pulses. By using the approach suggested in [37], the

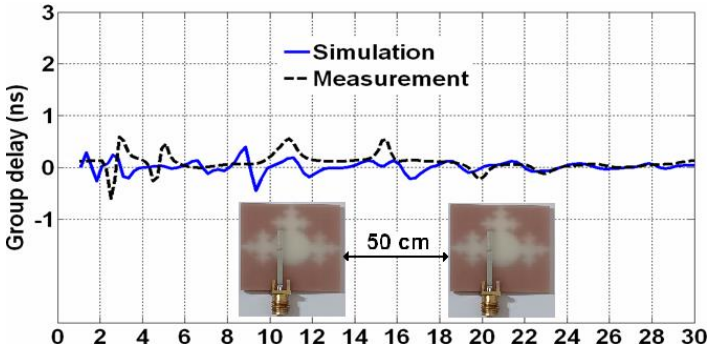

Fig. 8. Experimental and numerical group delay results of the antenna versus frequency.

input signal is delivered to the antenna, and the far-field electric component is received by means of seven virtual probes. To investigate the fidelity factor in both E- and H-plane, seven probes are placed at the angle equal to 0°, 15°, 30°, 45°, 60°, 75°, and 90° (with respect to positive z-axis) in x-z- and y-z-plane, respectively. In the numerical simulation procedure, the input signal was defined by a fourth-order Rayleigh pulse as follows:

$$s_t = \left(\frac{12}{\tau^2} - \frac{48}{\tau^6}(t-1)^2 + \frac{16}{\tau^8}(t-1)^4\right)\exp\left[-\left(\frac{t-1}{\tau}\right)^2\right] \tag{3}$$

with τ =67 ps. According to [38], the fidelity factor, *FF*, for the received pulse was calculated as follows:

$$FF = \max_k \int_{-\infty}^{\infty} \bar{s}_t(t)\bar{s}_r(t+k)dt \tag{4}$$

where $\bar{s}_t$ and $\bar{s}_r$ are the normalized transmitted and received pulses, respectively, and k is the constant delay time. Table II presents this time-domain parameter for both planes. In a typical UWB system, the values of fidelity factor can vary between 0 and 100%. A fidelity factor value of 0% shows that the received and input pulses are completely different from each other, while a value of 100% indicates that the received and input signals are perfectly similar. As was mentioned in [38], fidelity factor higher than 50% is appropriate value for UWB systems. From Table II, it is seen that the fidelity factor in both planes has satisfactory values greater than 77%, making the proposed antenna very capable for use in SWB communication systems. To calculate the FF, as mentioned in [38], the antenna gain and E-field phase should be calculated at every angle of the desired plane. Using the aforementioned parameters and transfer function of two identical antennas, like the procedure proposed in [38], the cross-correlation between both the received and the transmitted pulses is done at every point in time and the maximum value of this correlation is obtained. The FF in (4) has to be solved for every angle and plotted in a polar plot. Because of the normalization of the signals, the results of the cross-correlation are between 0 and 1.

Table II. Calculated fidelity factor of the antenna.

Angle (degrees)	**0**	**15**	**30**	**45**	**60**	**75**	**90**
Fidelity factor (E-plane) %	93	90	86	85	83	80	78
Fidelity factor (H-plane) %	94	92	88	85	81	78	77

Temperature humidity test chamber is able to simulate a wide range of temperature and humidity environments. It was used in testing fabricated antenna for its tolerances of heat, cold, dry and humidity. It was found that operating temperatures ranging from -45°C to +60°C, and humidity range is from 10% to 95% RH. These results show that the antenna can perform in environments with a wide range of operating temperatures and humidity

IV. CONCLUSION

In this research a compact planar SWB antenna with simple structure is presented. In order to jointly achieve compact structure with a SWB performance, fractal DGS on the ground plane is applied. The multi-frequency resonance characteristic and consequently SWB performance are obtained by increasing the fractal slots iterations on the ground plane. The antenna with electrical dimension of 0.11 λ× 0.11 λ provides BW ratio of 27.4:1 and operating BW of 186%. The novelty of the proposed antenna lies in its simple structure, compact size, high BDR, and SWB operation. The antenna has been simulated by full-wave Ansys Electromagnetics simulator package. The measured results of the fabricated prototype in frequency-and time-domain are also presented and compared with the simulated results. The peak-to-peak group delay variation of the antenna is less than 1ns over the entire frequency band and the antenna fidelity factor in both E- and H-planes has satisfactory values greater than 77. The performance of the designed antenna was compared with several recent SWB antennas. In spite of small electrical dimension of the antenna compare to the others, a large BDR of 15372 is provided. Hence, it can be concluded that the presented SWB antenna can provide good BW ratio and very larger BDR characteristics with much smaller size in comparison to the other antennas. Results indicate that the antenna provides excellent frequency- and time-domain performance without signal distortion. Therefore, the proposed antenna is very capable for use in SWB communication systems.

REFERENCES

[1] H. M. Bernety, B. Zakeri, R. Gholami, "Design of a novel directional microstrip-fed super-wideband antenna," *Modares Journal of Electrical Engineering*, vol. 11, no.3, pp. 2563-2570, Fall 2011.

[2] P. Okas, A. Sharma and R. Ku. Gangwar, "Super wideband CPW-fed modified square monopole antenna with stabilized radiation characteristics," *Microw. Opt. Technol. Lett*., vol. 60, pp. 568–575, Feb. 2018.

[3] D. Li and J.-F. Mao, “Sierpinskized koch-like sided multifractal dipole antenna,” *Progress In Electromagnetics Research*, vol. 130, pp. 207-224, 2012.

[4] S. S. Ghorpade, V. B. Babare and V. V. Deshmukh, “Comparison of E-shape Microstrip antenna and E-shape fractal antenna” *International Journal of Engineering Research and Technology (IJERT*), vol. 2, no. 4, pp. 2787-2790, Apr. 2013.

[5] K. Kharat, S. Dhoot and J. vajpai. “Design of compact multiband fractal antenna for WLAN and WiMAX Applications,” *IEEE, International conference on pervasive computing (ICPC)*, 2015.

[6] D. H. Werner, S. Ganguly, "An overview of Fractal Antenna Engineering Research", *IEEE Antennas and Propagation Magazine*, vol. 45, no. 1, pp. 38-57, Feb. 2003.

[7] J. Gianvittorio and Y. Rahmat-Samii, “Fractal element antennas: A compilation of configurations with novel characteristics,’’ *IEEE Antennas and Propagation Society International Symposium*, Salt Lake City, UT, USA, 16-21 July, 2000.

[8] M. N. Moghadasi, R.A. Sadeghzadeh, T. Aribi, T. sedghi, B.S. Virdee, “UWB monopole microstrip antenna using fractal tree unit-cells,” *Microwave and optical technology letters*, vol. 54, no. 10, pp. 2366–2370, July 2012.

[9] S. Singhal, P. Singh and A. K. Singh, “Asymmetrically CPW-FED Octagonal Sierpinski UWB Fractal Antenna,” *Microwave and Optical Technology letter*, vol. 58, no. 7, pp. 1738-1745, July 2016.

[10] D. Li, and J.-f. Mao, “A koch-like sided fractal bow-tie dipole antenna,” *IEEE Trans. Antennas Propag*., vol. 60, no. 5, pp. 2242-2251, May 2012.

[11] Y.-W. Zhong, G.-M. Yang, and L.-R. Zhong, “Gain enhancement of bow-tie antenna using fractal wideband artificial magnetic conductor ground,” *Electron. Lett*., vol. 51, no. 4, pp. 315-317, Feb. 2015.

[12] S. Kumar Terlapu, Ch. Jaya and G.S. Raju, “On the Notch Band Characteristics of Koch Fractal Antenna for UWB Applications,” *International Journal of control theory and applications*, vol. 10, no. 6, pp. 701-707, Apr. 2017.

[13] M. A. Dorostkar, M. T. Islam, and R. Azim, "Design of A Novel Super Wide Band Circular-Hexagonal Fractal Antenna," *Progress In Electromagnetics Research*, Vol. 139, 229-245, 2013.

[14] B. L. Shahu, S. Pal, and N. Chattoraj, "Design of Super Wideband Hexagonal-Shaped Fractal Antenna With Triangular Slot," *Microwave and Optical Technology Letters*, vol. 57, no. 7, pp. 1659-1662, July 2015.

[15] V. Waladi, N. Mohammadi, Y. Zehforoosh, A. Habashi and J. Nourinia, “A Novel Modified Star-Triangular Fractal (MSTF) Monopole Antenna for Super-Wideband Applications,” *IEEE Antennas and Wireless Propagation Letters*, vol. 12, pp. 651-654, May 2013.

[16] A. Tanweer, B. K. Subhash, and C. B. Rajashekhar, “A miniaturized decagonal sierpinski UWB fractal antenna,” *Progress In Electromagnetics Research C*, vol. 84, 161-174, 2018.

[17] H. Tizyi, F. Riouch1, A. Tribak1, A. Najid1, and A. Mediavilla, “CPW and microstrip line-fed compact fractal antenna for UWB-RFID applications,” *Progress In Electromagnetics Research C*, vol. 65, 201–209, 2016.

[18] W. Balani, M. Sarvagya, T., MM, M. P. Ali, J. Anguera, A. Andujar, and S. Das, “Design techniques of super-wideband antenna-Existing and future prospective,” *IEEE Access*, vol. 7, pp. 141241-141257, 2019.

[19] A. Dastranj, F. Ranjbar, and M. Bornapour, “A New Compact Circular Shape Fractal Antenna for Broadband Wireless Communication Applications,” *Progress In Electromagnetics Research C*, vol. 93, pp. 19-28, 2019.

[20] A. Dastranj, G. Lari, and M. Bornapour, “A compact dual band-notched SWB antenna with high bandwidth dimension ratio,” *International Journal of Microwave and Wireless Technologies*, vol. 13, no. 1, pp. 87–93, 2021.

[21] J. Yeo, and J. I. Lee, “Coupled-sectorial-loop antenna with circular sectors for super wideband applications,” *Microw Opt Technol Lett*., vol. 60, pp. 1683–1689, Apr. 2014.

[22] S. Hakimi, S. K. A. Rahim, M. Abedian, S. Noghabaei and M. Khalily, A.K. Singh, “CPW-fed transparent antenna for extended ultrawideband applications,” *IEEE Antennas Wireless Propag. Lett.*, vol. 13, pp. 1251-1254, June 2016.

[23] S. Singhal and A. K. Singh, "CPW-fed hexagonal sierpinski super wideband fractal antenna," *IET Microw. Antennas Propag*., vol. 10, no. 15, pp. 1701-1707, Dec. 2016.

[24] K. R. Chen, C. Sim, J. S. Row "A compact monopole antenna for super wideband applications," *IEEE Antennas Wireless Propag. Lett.*, vol. 10, pp. 488–491, May 2011.

[25] B. L. Shahu, S. Pal, N. Chattoraj "Design of super wideband hexagonal-shaped fractal antenna with triangular slot," *Microw. Opt. Technol. Lett*., vol. 57, no. 7, pp. 1659–1662, July 2015.

[26] C. Deng, Y. J. Xie, and P. Li, "CPW-fed planar printed monopole antenna with impedance bandwidth enhanced," *IEEE Antennas Wireless Propag. Lett.*, vol. 8, pp. 1394–1397, 2009.

[27] M. N. Srifi, S. K. Podilchak, M. Essaaidi, and Y. M. M. Antar, "Compact disc monopole antennas for current and future ultrawideband (UWB) applications," *IEEE Trans. Antennas Propag.*, vol. 59, no. 12, pp. 4470–4480, Dec. 2011.

[28] S. Cheng, P. Hallbj¨ orner, and A. Rydberg, "Printed slot planar inverted cone antenna for ultrawideband applications," *IEEE Antennas Wireless Propag. Lett.*, vol. 7, pp. 18–21, 2008.

[29] A. Azari, "A new super wideband fractal microstrip antenna," *IEEE Trans. Antennas Propag.*, vol. 59, no. 5, pp. 1724–1727, May 2011.

[30] Y. Dong, W. Hong, L. Liu, Y. Zhang, and Z. Kuai, "Performance analysis of a printed super wideband antenna," *Microw. Opt. Technol. Lett*., vol. 51, no. 4, pp. 949–956, Apr. 2009.

[31] J. Liu, K. P. Esselle, S. G. Hay, and S. Zhong, "Achieving ratio bandwidth of 25 : 1 from a printed antenna using a tapered semi-ring feed," *IEEE Antennas Wireless Propag. Lett.*, vol. 10, pp. 1333–1336, 2011.

[32] S. Singhal and A. K. Singh, "CPW-fed phi-shaped monopole antenna for super wide-band applications," *Progress in Electromagnetics Research.*, vol. 64, pp. 105–116, 2016.

[33] A. Dastranj, "Low-profile ultra-wideband polarisation diversity antenna with high isolation," *IET Microwaves, Antennas Propag*.," vol. 11, no. 10, pp. 1363-1368, Aug. 2017.

[34] A. Dastranj, "Modified end-fire bow-tie antenna fed by microstrip line for wideband communication systems," *Journal of Electromagnetic Waves and Applications*, vol. 32, no. 13, pp. 1629-1643, May 2018.

[35] A. Dastranj and M. Bornapour, "UWB planar conical horn-shaped self-complementary bow-tie antenna," *Journal of Communication Engineering (JCE)*, vol. 8, no 1, pp. 20-33, winter and spring 2019.

[36] A. Dastranj and Z. Javidi, "A Multi-Band Asymmetric Stepped-Slot Antenna for DCS, PCS, WiMAX, 4G, and WLAN Applications," *Journal of Communication Engineering (JCE)*, vol. 8, no 1, pp. 9-20, January-June 2020.

[37] Q. Wu, R. Jin, J. Geng, and M. Ding, "Pulse preserving capabilities of printed circular disk monopole antennas with different grounds for the specified input signal forms," *IEEE Trans. Antennas Propag.*, vol. 55, no. 10, pp. 2866–2873, Oct. 2007.

[38] Quintero, G., Zurcher, J. F., Skrivervik, A. K., 'System fidelity factor: A new method for comparing UWB antennas," *IEEE Trans. Antennas Propag*., vol. 59, no. 7, pp. 2502–2512, July 2011.